Supporting Information:

Enhanced Vertical Concentration Gradient in Rubbed P3HT:PCBM Graded Bilayer Solar Cells

By *Varun Vohra**, *Gianmichele Arrighetti, Luisa Barba, Koichi Higashimine*, *William Porzio* and *Hideyuki Murata**

In the supporting information, we provide further characterization of the unrubbed and rubbed films of P3HT as well as devices based on these films.

In a first place, we provide the photoelectron yield spectroscopy (PYS) spectra measured using an AC-2 system from Riken Keiki. The spectra include the lines used as baseline and regression line. The crossing point of these two lines gives us information about the location of the HOMO level of the material before and after treatment (**Figure SI1**). It is worth mentioning that PYS only probes the surface of the measured samples which, however, demonstrates the influence of the chain orientation on the energetic level of P3HT.

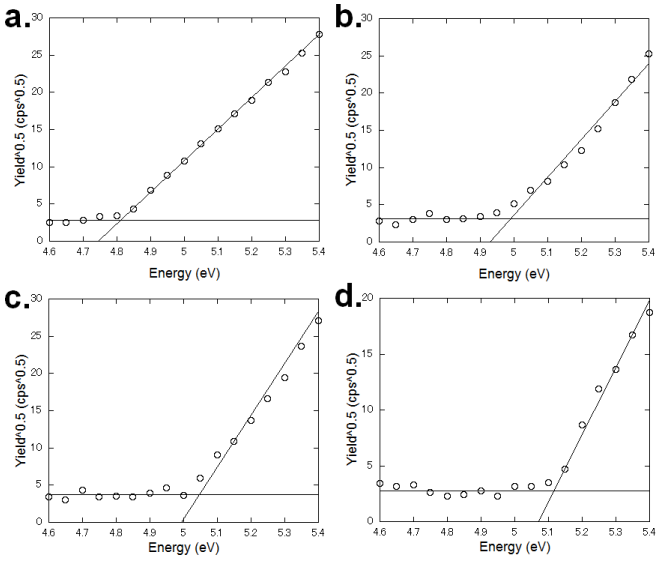

Figure SI1. PYS spectra obtained for 0 (a). 3 (b), 5 (c) and 10 (d) times rubbed P3HT layers prior to PCBM deposition.

The study of the rubbing process over the surface morphology of the thin films is studied by AFM. **Figure SI2** displays the evolution of the surface morphology upon rubbing 3, 5 and 10 times. AFM images were obtained using a Nanoscale Hybrid Microscope VN-8000 from Keyence and further analyzed using the VN-Analyzer program provided by Keyence.

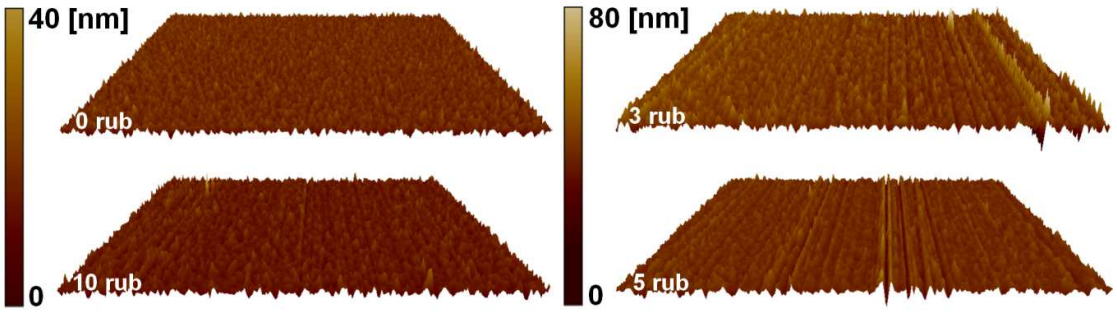

Figure SI2. 3D AFM images of 0, 3, 5 and 10 times rubbed P3HT films. The images correspond to an area of 50 μm x 50 μm.

Rubbing times	0	3	5	10
RMS	4.9	4.6	5.0	4.4
Rz (nm)	24.4	39.4	49.6	24.3

Table SI1. summary of the surface roughness analysis of the unrubbed and rubbed samples

AFM images were obtained using a Nanoscale Hybrid Microscope VN-8000 from Keyence. Unlike the 10 times rubbed films, the 5 times rubbed P3HT displays gratings which reach up to 50 nm of height. The thickness of the spin coated PCBM being 40 nm, due to structure planarization, there is a high probability that some P3HT can still be detected in the top 5 nm of the film after PCBM deposition which explains the edge-on crystallites observed in the 5 times rubbed films. The unrubbed and 10 times rubbed films, on the other hand, do not have any features with heights over 25 nm and therefore the whole P3HT films are covered by at least 15 nm of PCBM.

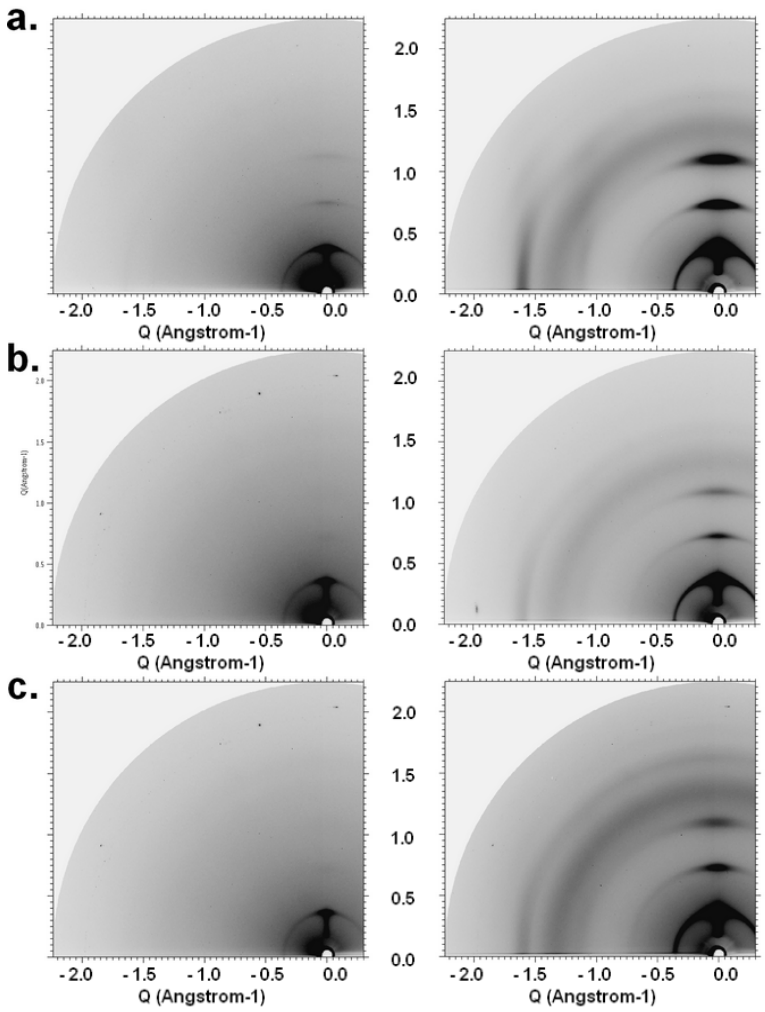

Figure SI3. Grazing (left) and incident (right) XRD images obtained for (a) 0, (b) 5 and (c) 10 times rubbed active layers. The used wavelength is 0.12 nm. The calculated scattering depth is 5 and 550 nm in grazing and incidence conditions respectively.[SI1]

Figure SI2 displays the results obtained in the GI-XRD measurements for all the measured films and, along with **Table SI2** below, provides complementary information to **Figure 2**. This Table is the extension of Fig. 1c, allowing to estimate the crystallite perfection of P3HT layer, according to Hosemann paracrystal theory. [SI2]

Table SI2. Results of GI-XRDD profile analysis of films P3HT/PCBM .

Profile type	*OP*						*IP*			
sample[a]	d_{100}[b]	$L_{(100)}$[c]	$g_{100/200}$	$g_{200/300}$	$d_{(020)}$	L[c]	$d_{(020)}$[c]	L	$d_{(100)}$	L
x10 graz	1.64	11,5	4.7	4.3	0,382	3,5	0,376	4,5	1,665	11,5
x10 inc	1.6	15	5.0	4.1	0,376	5,5	0,378	5,5	1,64	14
x5 graz	1.6	19	4.6	3.4	-	-	0,374	7	1,61	11
x5 inc	1.6	19	4.8	3.8	0,379	4.50	0,382	4,6	1,64	16,5
no-rub graz	1.6	12,5	5.8	3.6	0,375	4.2	0,376	4,5	1,64	17
no-rub inc	1.6	16	4.8	4.1	0,375	4.8	0,378	5	1,64	14,5

[a] The labels mean the rubbing times and the incidence angles 0.05° (grz) and 0.15° (inc), respectively. The $d_{[h\,0\,0]}$ correction for refraction effects was applied (for the incidence angle chosen ~ $5 \cdot 10^{-2}$ nm) [SI3]. Pseudo-Voigt mixing parameter (η) has been optimized [SI4, SI5], ranging from 0.45 to 0.55.
[b] The spacing values (nm) are averaged along with the observed orders.
[c] L is the average crystallite dimension as derived from ref. 3. The estimated standard deviation (e.s.d.) is <1 nm.

[e] The g_{hkl} is the lattice fluctuation factor, which e.s.d. is <0.25, according to Hosemann paracrystal theory [SI2]
[f] The $d_{(020)}$ and related crystallite dimension L are observed in OP profile.
[h] The $d_{(100)}$ and related crystallite dimension L are observed in IP profile.

The q resolution of 2D images collected was estimated by means of Lanthanum hexaboride powder (standard reference material 660a of NIST) in 2-θ range < 50° and it has been evaluated better than 0.25 mrad both for q_z and q_{xy}, in agreement with other synchrotron measurements [SI6]. $d_{[h\,0\,0]}$ correction for refraction effects was applied (for the incidence angle chosen ~5 x 10^{-2} nm).[SI6] Pseudo-Voigt mixing parameter (η) has been optimized [SI6], ranging from 0.45 to 0.55. The spacing values (nm) are averaged along with the observed orders. L is the average crystallite dimension as derived from [SI4]. The estimated standard deviation (e.s.d.) is <1 nm.

In the 5 times rubbed films, we detect large amounts of edge-on P3HT crystallites close to the surface. Unlike the face-on crystallites observed in unrubbed films, these crystallites do not result from P3HT dissolution during the process. Due to structure planarization during spin-coating of the 40 nm thick PCBM layer, part of the gratings created in the 5 times rubbed films (Rz = 49.6 nm, **Table SI1**) may still be detected through radial GI-XRD measurements. The reduction of face-on crystallites at the surface as well as the increase of crystallinity and face-on to edge-on ratio observed for the 10 times rubbed films is also observed in the 5 times rubbed films confirming that molecular reorientation and better vertical concentration gradients are not only found in 10 times rubbed films but also in the 5 times rubbed ones.

Even though the rubbing process induces some positive changes at the molecular level in P3HT films, it also generates some defect when it comes to the homogeneity of the films.

We note that the images in the main text (**Figure 3**) correspond to the parts of the active layer with no defects. Thinner parts of less than 50 nm, corresponding to defects resulting from the rubbing process, do not show any relevant concentration gradient. **Figure SI3** displays a few examples of thinner active layers resulting from the rubbing process. In these thinner parts, no particular concentration gradient is observed and we remain in a situation very similar to a bulk heterojunction. These defects slightly affect the device performances and are the main reason for the changes in device performances for devices obtained with the same number of rubbings.

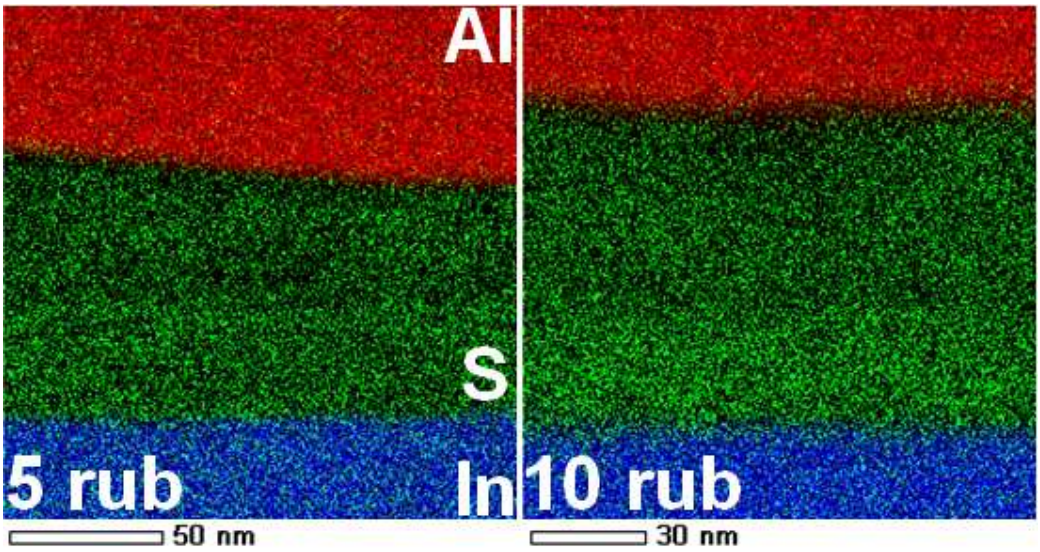

Figure SI4: EDS element mapping of cross-section of thinner active layers in 5 and 10 times rubbed active layers.

Experimental Details:

P3HT (Mw = 21 000 g.mol^{-1}), PCBM and PEDOT:PSS (Clevios P) were purchased from Merck, Luminescence Technology Corp and H.C.Starck, respectively. Glass substrates coated with 150 nm thick ITO layers are used as the anode. After a standard cleaning procedure and

exposure to UV irradiation, they are covered with 35 nm of PEDOT:PSS (4000 rpm for 60s, annealed at 200˚C for 10 min).

The current–voltage characteristics of the encapsulated devices were measured in air, using a Keithley 2400 Sourcemeter and a Solar simulator at one sun light irradiance (AM 1.5, 100mW/cm^2) at room temperature. Photoelectron Yield Spectra were measured using a AC-2 Spectrometer from Riken Keiki.

GI-XRD has been carried out at room temperature at the XRD1 beamline of the ELETTRA synchrotron facility (Trieste, Italy) using a 10.34 keV monochromatic beam (0.12 nm). The X-ray incidence angle (α_i) on the sample ranged from 0.02° to about 1° and a 2D-CCD camera (MAR research camera of 165 mm diameter and 79.168 µm pixel size) was placed normal to the incident beam direction at a distance of 180 mm from the sample to record the diffraction pattern in reflection mode. Sample and detector were kept fixed during the measurements. A detailed procedure of diffraction data treatment together with the line profile analysis of spectra extracted from the two-dimensional images both in in-plane (IP) and in out-of-plane (OP) geometry has been previously reported.[SI6] The q resolution of 2D images collected was estimated by means of Lanthanum hexaboride powder (standard reference material 660a of NIST) in 2-θ range < 50° and it has been evaluated better than 0.25 mrad both for q_z and q_{xy}, in agreement with other synchrotron measurements [SI3, SI6]. The grazing (graz) and incident (inc) angles are 0.05° and 0.15°, respectively.

EDS for elemental analysis was carried out with a scanning transmission electron microscope, JEM-ARM200F from JEOL. The acceleration voltage and probe current were 200 kV and 59 pA, respectively to obtain 256 x 256 pixels images with a dwell time of 1 ms/pixel. Each image was accumulated for 120 s to improve the signal to noise ratio. (No rubbed samples for 60 s).

REFERENCES (Supporting Information)

[SI1] Dosch, H.; Battermann, B.W.; Wack, D.C. Depth-controlled grazing-incidence diffraction of synchrotron x radiation. *Phys. Rev. Lett.* **1986**, *56*, 1144–1147.

[SI2] Hindeleh, A.M.; Hosemann, R. Microparacrystals: the intermediate state between crystalline and amorphous. *J. Mater. Sci.* **1991**, *19*, 5127–5136 and ref. therein.

[SI3] Lilliu, S.; Agostinelli, T.; Pires, E.; Hampton, M.; Nelson, J.; Macdonald, J.M. Dynamics of Crystallization and Disorder during Annealing of P3HT/PCBM Bulk Heterojunctions. *Macromolecules* **2011**, *44*, 2725-2734.

[SI4] Enzo, S.; Fagherazzi, G.; Benedetti, A.; Polizzi, S. A profile-fitting procedure for analysis of broadened X-ray-diffraction peaks. 1. Methodology. *J. Appl. Cryst.* **1988**, *21*, 536–540.

[SI5] Rivnay, J.; Noriega, R.; Kline, R.J.; Salleo, A.; Toney, M.F. Quantitative analysis of lattice disorder and crystallite size in organic semiconductor thin films. *Phys. Rev. B* **2011**, *84*, 045203.

[SI6] Porzio, W.; Scavia, G.; Barba, L.; Arrighetti, G.; Milita, S. Depth-Resolved Molecular Structure and Orientation of Polymer Thin Films by Synchrotron X-ray Diffraction. *Eur. Polym. J* **2011**, *47*, 273-283 and ref. therein.